International Journal of Architectural, Civil and Construction Sciences
ISSN: 2415-1734
Vol:10, No:6, 2016

Seismic Performance Assessment of Pre-70 RC Frame Buildings with FEMA P-58

D. Cardone

***Abstract*—**Past earthquakes have shown that seismic events may incur large economic losses in buildings. FEMA P-58 provides engineers a practical tool for the performance seismic assessment of buildings. In this study, FEMA P-58 is applied to two typical Italian pre-1970 reinforced concrete frame buildings, characterized by plain rebars as steel reinforcement and masonry infills and partitions. Given that suitable tools for these buildings are missing in FEMA P-58, specific fragility curves and loss functions are first developed. Next, building performance is evaluated following a time-based assessment approach. Finally, expected annual losses for the selected buildings are derived and compared with past applications to old RC frame buildings representative of the US building stock.

***Keywords*—**FEMA P-58, RC frame buildings, plain rebars, masonry infills, fragility functions, loss functions, expected annual loss.

I. Introduction

IN the probabilistic framework of FEMA P-58 [1], estimation of economic losses is performed in four steps. In the first step, the structural response at increasing levels of seismic hazard is defined by a series of simulated demand sets generated either by computer simulation analyses or simplified approaches. In the second step, expected damage to individual structural and nonstructural components is estimated, from a probabilistic perspective. In the third step, economic losses to individual components are evaluated as a function of the level of damage suffered by each component. Finally, economic losses to individual components are aggregated at the building level, to provide a number of performance measures (e.g. repair cost, repair time and casualties) useful to quantify the consequences associated with earthquake damage. Step 2 of FEMA P-58 requires the use of suitable fragility functions. Similarly, step 3 requires the definition of a set of suitable consequence functions able to translate damage into potential repair/replacement costs, repair time and casualties for the building under scrutiny.

FEMA P-58 includes a large database of fragility curves and consequence functions for different categories of structural and non-structural components, which are typical for US buildings, but that essentially are not valid for many other building types worldwide. Therefore, further efforts are needed in the attempt to extend the applicability of the FEMA P-58 methodology.

The main objective of this study is to apply the FEMA P-58 methodology to older Reinforced Concrete (RC) buildings representative of those realized in Italy (and other European countries) before 1970 (i.e. before the introduction of seismically oriented codes). The building type under consideration includes RC frame buildings designed for gravity loads only, using low-strength concrete and plain steel reinforcing bars, and featuring masonry infills as non-structural exterior walls and internal partitions. At the moment, specific tools (i.e. fragility curves and loss functions) for the seismic performance evaluation of such buildings are missing. For that reason, preliminary efforts have been made to develop fragility curves and consequence functions specific for the main structural and non-structural components of the buildings under consideration.

The paper is organized in two parts. In the first part, fragility and loss parameters are briefly presented in a format suitable to be implemented in PACT (Performance Assessment Calculation Tool) of FEMA P-58 for performance seismic assessment. In the second part, the results derived from the application of the FEMA P-58 to two case study buildings are presented. Finally, the Expected Annual Loss (EAL) for the selected buildings is compared with results from past applications to old RC frame buildings representative of the US building stock.

II. Fragility and Loss Functions

In this section, fragility curves and loss functions developed in this study for typical structural and non-structural components of pre-70 RC frame buildings are briefly presented. More details on the methodology followed to derive fragility curves and loss functions, including references and experimental data, can be found in [2], [3]. The Fragility Groups (FGs) of RC structural components and non-structural masonry walls considered in this study are listed in the first column of Tables I, II. Damage states and associated repair methods are summarized in Tables III, IV.

Fragility functions have been developed summarizing results from previous experimental tests on laboratory specimens with design details representative of typical pre-70 RC frame buildings. The interstorey (or column) drift ratio (IDR/CRD) has been chosen as engineering demand parameter. Fragility functions have been evaluated assuming a lognormal distribution for the collected experimental data, with median value θ_i and logarithmic standard deviation (i.e. dispersion) β_i evaluated according to the procedure described in the Appendix H of FEMA P-58.

The fragility parameters implemented in PACT for damage assessment of RC components and masonry infills and partitions are summarized in Tables I and II, respectively.

D. Cardone is with University of Basilicata, 85100 Potenza, Italy, (e-mail: donatello.cardone@unibas.it).

TABLE I
FRAGILITY AND LOSS PARAMETERS FOR RC STRUCTURAL COMPONENTS

Fragility Groups	Damage State	Fragility parameters θ_i (%)	β_i	Loss parameters $\lambda_{FGj,DSi}$	$\beta_{FGj,DSi}$	λ_{max}	λ_{min}	q_{max}	q_{min}
External Weak Joints (EWJ)	DS1	0.75%	0.40	0.74	0.45	0.96	0.59	20	5
	DS2	1.25%	0.40	1.16	0.40	1.39	0.99	20	5
	DS3	2.00%	0.40	1.57	0.42	1.88	1.33	20	5
Internal Weak Beams (IWB)	DS1	0.65%	0.40	0.48	0.46	0.62	0.38	20	5
	DS2	1.75%	0.35	0.78	0.41	0.93	0.66	20	5
	DS3	3.00%	0.30	1.22	0.42	1.46	1.03	20	5
Internal Weak Columns (IWC)	DS1	0.75%	0.40	0.53	0.46	0.69	0.43	20	5
	DS2	1.75%	0.35	0.77	0.38	0.92	0.65	20	5
	DS3	3.0%	0.35	1.01	0.42	1.21	0.86	20	5
Ductile Weak Columns (DWC)	DS1	0.75%	0.40	0.67	0.47	0.88	0.54	20	5
	DS2	1.25%	0.40	0.99	0.37	1.19	0.85	20	5
	DS3	2.00%	0.40	1.25	0.41	1.50	1.07	20	5

TABLE II
FRAGILITY AND LOSS PARAMETERS FOR MASONRY INFILLS AND PARTITIONS

Fragility Group	Damage States	Fragility parameters θ_i IDR (%)	β_i	Loss parameters $\lambda_{FGj,DSi}$	$\beta_{FGj,DSi}$	λ_{max}	λ_{min}	q_{max}	q_{min}
External Infill Walls (EIW)	DS1	0.15%	0.5	0.19	0.22	0.24	0.15	20	5
	DS2	0.40%	0.5	0.40	0.44	0.48	0.34	20	5
	DS3	1.0%	0.4	1.90	0.44	2.28	1.61	20	5
	DS4	1.75%	0.35	1.92	0.52	2.30	1.64	20	5
External Infill Walls with windows (EIW_w)	DS1	0.10%	0.5	0.19	0.30	0.24	0.15	20	5
	DS2	0.30%	0.5	0.34	0.46	0.41	0.29	20	5
	DS3	0.75%	0.4	1.30	0.46	1.56	1.10	20	5
	DS4	1.75%	0.35	1.44	0.52	1.73	1.22	20	5
External Infill Walls with French windows (EIW_fw)	DS1	0.075%	0.5	0.17	0.28	0.22	0.13	20	5
	DS2	0.20%	0.5	0.32	0.46	0.39	0.27	20	5
	DS3	0.50%	0.4	1.32	0.46	1.58	1.12	20	5
	DS4	1.75%	0.35	1.55	0.52	1.86	1.31	20	5
Internal Partitions (IP)	DS1	0.15%	0.5	0.22	0.19	0.28	0.17	20	5
	DS2	0.40%	0.5	0.43	0.45	0.52	0.37	20	5
	DS3	1.0%	0.4	1.96	0.45	2.35	1.66	20	5
Internal Partition with doors (IP_d)	DS1	0.075%	0.35	0.18	0.25	0.24	0.15	20	5
	DS2	0.20%	0.5	0.34	0.46	0.41	0.29	20	5
	DS3	0.50%	0.5	1.40	0.46	1.68	1.19	20	5

TABLE III
DAMAGE STATES OF RC COMPONENTS AND ASSOCIATED REPAIR ACTIONS

Damage States	Damage Description	Repair Actions
DS1	Light cracking	Epoxy injection of concrete cracks
DS2	Severe cracking, spalling of cover concrete	Patch concrete with mortar mix
DS3	Crushing of concrete, possible buckling of rebars	Replace concrete (and rebars, if necessary)

TABLE IV
DAMAGE STATES OF MASONRY INFILLS AND ASSOCIATED REPAIR ACTIONS

Damage states	Damage Description	Repair Actions
DS1	Detachment of infill, light diagonal cracking	Patch some cracks
DS2	Extensive diagonal cracking, possible failure of brick units.	Patch cracks and restore loose masonry
DS3	Corner crushing and sliding of mortar joints	Demolish existing wall and construct new wall. Re-install existing frame (if any)
DS4	In-plane or out-of-plane collapse	Demolish existing wall and construct new wall. Install new frame (if any)

To derive loss functions, each damage state has been univocally associated with a specific set of repair actions (see Tables III, IV). Repairing also includes a number of preliminary/supplementary activities (e.g. access protection, arrangement of dust curtains, installation of scaffolding and shoring systems, removal of furnishings and floor finishes, demolition of portions of infills and partitions, isolation of possible plumbing/wiring systems, removal of debris, replacement/restoring of furnishings, partitions, floor finishes, plumbing/wiring systems, etc.) that have been considered in the development of loss functions. Next, the unit costs for the repair works envisaged for every damage state of each fragility group have been estimated based on official costing manuals for Italy. Then, normalized repair cost ratios ($L_{FGj,DSi}$ in Tables I, II) have been derived, based on quantity survey of a number of pre-70 RC buildings. Cumulative lognormal distributions of the total repair cost ratios have been then derived, estimating 10^{th} and 90^{th} percentile levels based on engineering judgment. The resultant median $\lambda_{FGj,DSi}$ and dispersion $\beta_{FGj,DSi}$ are reported in Tables I, II for each FG and DS. Loss functions to be implemented in PACT have been finally derived assuming, in line with the FEMA P-58, suitable maximum/minimum normalized total repair cost ratios $\lambda_{max}/\lambda_{min}$ and associated lower/upper quantities of components (q_{min}/q_{max}) below/above which there is no discount reflecting economies of scale or efficiencies in operation (see Tables I, II).

III. CASE STUDIES

The Reinforced Concrete (RC) frame buildings examined in this study include three archetype buildings, with number of storeys ranging from 4 to 8 (labeled with 4A, 6A, 8A), and a real 8-storey building (labeled with 8R). The selected buildings are representative of typical residential buildings realized in Italy before '70s.

The archetype buildings feature 27.0 ×15.0 m plan dimensions and 3.0 m interstorey height. All the archetype buildings have the same structural configuration (with internal frames in the long direction only), while differing in the dimensions of the columns along the height of the building.

The real building, is represented by an existing building built in 1962 in the city of Potenza (southern Italy), with 26.75 ×12.40 m plan dimensions and 3.16 m interstorey height (except for the first storey where the interstorey height is 4.6 m). The structural configuration of the real building differs from that of the archetype buildings, due to presence of internal frames in the short direction only. All the buildings feature a dog-leg stair with cantilever steps sustained by two stiff 'knee' beams.

The structural characteristics of the archetype buildings (geometric dimensions, reinforcement ratios, structural details, etc.) have been derived from a simulated design, considering gravity loads only, according to the technical standard and state of practice enforced in Italy before '70s. Reference to the original design documents has been made for the real building.

Cross section dimensions and reinforcement ratios of beams and columns are summarized in Table I for each building under consideration.

Steel reinforcement is realized with smooth steel rebars with end-hooks in the exterior beam-column joints and at the base of the columns. As far as the strength of materials is concerned, an average compression strength of 25 MPa and a yield strength of 325 MPa have been assumed for concrete and steel, respectively.

Finally, the buildings feature external infills made of hollow clay bricks arranged in two single walls of 100 mm thickness each, separated by a cavity of 100 mm. Internal partitions are realized with a single layer of hollow clay bricks with 100 mm thickness.

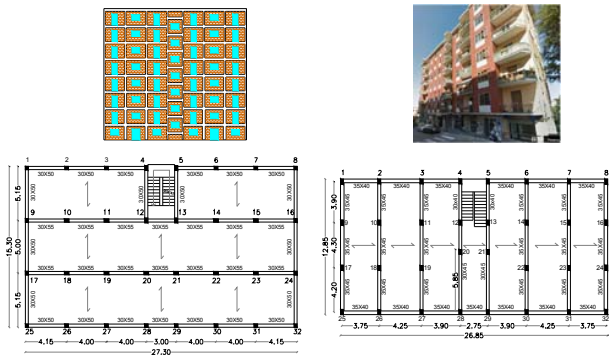

(a) (b)

Fig. 1 Examined (a) archetype and (b) real buildings.

TABLE V
CHARACTERISTICS OF THE EXAMINED CASE STUDIES

Case Study	Column section (cm)	Beam section (cm)	Reinforcement ratios	Replacement Cost (€)
4A	E: 30×35÷30×30 I: 30×45÷30×35 C: 30×30	E: 30×50 I: 30×55 KB: 30×50	Beams: 0.56% ÷ 0.71% Columns: 0.59% ÷ 0.68%	927655
6A	E: 30×45÷30×40 I: 30×55÷30×35 C: 30×30	E: 30×50 I: 30×55 KB: 30×50	Beams: 0.56% ÷ 0.71% Columns: 0.59% ÷ 0.75%	1391483
8A	E: 30×55÷30×30 I: 30×65÷30×35 C: 30×30	E: 30×50 I: 30×55 KB: 30×50	Beams: 0.56% ÷ 0.71% Columns: 0.59% ÷ 0.79%	1855311
8R	(I-II storey: 40×60) E: 25×30÷28×50 I: 25×30÷28×45 C: 28×30÷28×50	E: 35×40÷40×55 I: 30×40÷40×55 KB: 28×30	Beams: 0.39% ÷1.28% Columns: 0.60% ÷1.13%	2380100

E: External; I: Internal; C: corner; KB: knee beams

In the last column of Table V, the Replacement Cost (RepC) of each building model is reported. RepC has been estimated based on the current (2014) average construction cost per square meter for new residential buildings with similar volume and characteristics (equal to 730 €/m^2 according to [4]). An additional cost of 44 €/m^3 has been considered to account for demolition and disposal activities.

For simplicity, all the buildings are supposed to be located in the city of L'Aquila (central Italy), which is characterized by the highest levels of seismic hazard for Italy (0.452 g PGA with 2475 years return period on stiff soil). Reference to the data provided by the INGV (Italian Institute of Geophysics and Volcanology) for the city of L'Aquila (Italy), soil type A, has been made to derive the hazard curves for each building model (see Fig. 2), considering the relevant differences in terms of average fundamental period of vibration T*.

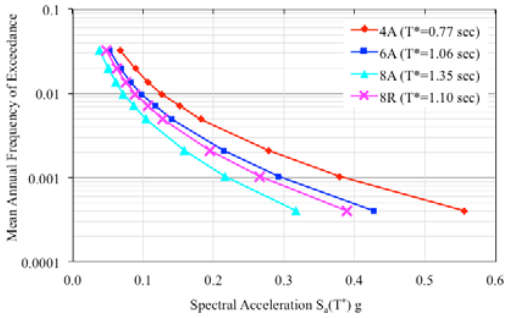

Fig. 2 Hazard Curves for the selected case studies

IV. BUILDING PERFORMANCE MODEL

A refined 3D lumped plasticity model has been implemented in SAP2000_Nonlinear, to accurately describe the seismic behavior of the selected case-study buildings and their possible failure modes. In particular, plastic hinges of beams and columns have been modeled with multi-linear plastic pivot NLlink elements, whose skeleton curve has been derived from moment-curvature analysis of the critical cross section, taking into account axial load interaction and bar slipping effects. Possible brittle shear failure of the short columns around the staircase has been captured with in-series shear springs with post-cap degrading behavior. Exterior beam-column joints have been also described with a moment-rotation NLlink elements with post-peak degrading behavior, in accordance with the model by [5]. Exterior masonry infills have been modeled with an equivalent compression-only triple-strut model, featuring a three-linear skeleton curve described by a revised Decanini model [6]. The influence of openings (windows, doors and French windows) and possible premature out-of plane collapse modes of masonry infills, have been also taken into account. More details on modeling assumptions and model parameters can be found in [7].

Loss assessment of the selected buildings has been performed with PACT, following the time-based performance assessment methodology described in FEMA P-58, considering nine different seismic intensities, with return periods ranging from 30 to 2475 years. Nonlinear Time History Analyses (NTHA) have been performed using nine sets of ten ground motion pairs, compatible with Conditional Mean Spectra [8], considering the M-R-ε (Magnitudo-Distance-Deviation) disaggregation and a proper attenuation relationship for the city of L'Aquila. For each ground motion pair, the maximum absolute values of interstorey drifts and story accelerations have been determined and used as input in PACT to generate simulated demand sets.

Different performance groups of vulnerable structural and non-structural components have been identified (see Table VI). Specific fragility and loss functions have been then derived for the main structural and non structural components of pre-70 RC frame buildings, including external and internal beam-column joints, ductile and brittle weak columns, masonry infills with and without openings [2,3]. PACT analyses have been performed considering 500 realizations for each seismic intensity, assuming uncorrelated fragility groups and different values of total loss thresholds, ranging from 0.4 to 1.

Collapse fragility functions have been evaluated, based on results of Pushover Analysis, with the SPO2IDA (Static Pushover to Incremental Dynamic Analysis) tool provided in PACT, assuming a lognormal dispersion of 0.6. Building repair has been deemed to be economically and practically not feasible when residual drifts exceeded 1%. Therefore, a lognormal residual drift fragility function with median value of 1% and dispersion of 0.3 has been assumed.

TABLE VI
FRAGILITY GROUPS CONSIDERED IN THE PERFORMANCE ASSESSMENT

Performance Groups	Fragility Groups	Reference
External beam-column joints	Weak joints, beam flexural response	[3]
Internal beam-column joints	Weak beams, column flexural response	
	Weak columns, beam flexural response	
	Weak columns, strong joints (e.g. base columns)	
Columns	Not ductile columns (e.g. short columns around staircase)	
Exterior walls	Masonry infills	
Exterior walls with openings	Masonry infills with window	
	Masonry infills with French window	
Interior walls	Masonry partitions	
Interior walls with openings	Masonry partitions with door	
Electrical service and distribution	(DS2-DS4) Masonry infill walls	[2]
Ceramic tiles		
Water and sanitary system		
Skirting		
Sanitary Ware and Plumbing fixtures		
Windows	(DS3-DS4) Masonry infill walls	
French Windows		
Doors		
External Scaffolding	(DS1) Masonry infill Walls	[1]
Roof coverings	Unsecured clay tiles	
Chimney	Masonry chimneys	
Lighting	Independent pendant lightings	
Piping	Cold water piping	
	Hot water piping	
	Sanitary waste piping	

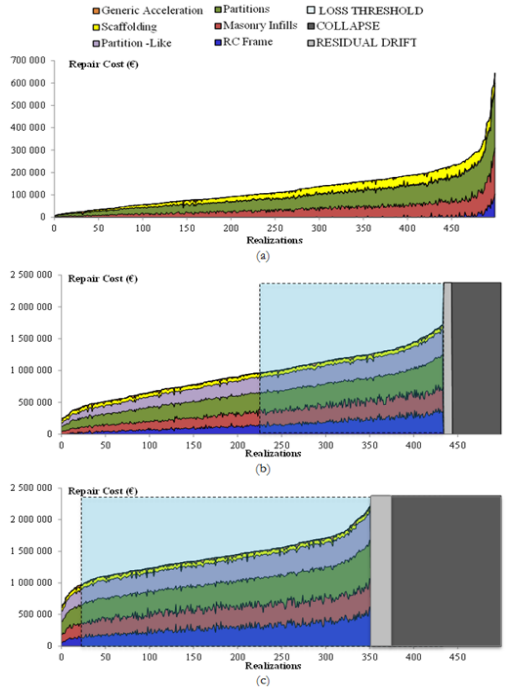

Fig. 3 Repair costs experienced by the 8-storey real building at (a) IM1, (b) IM7 and (c) IM8

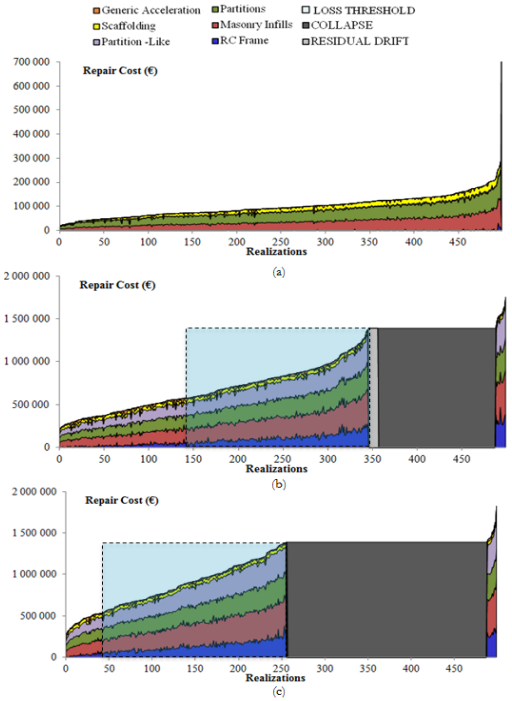

Fig. 4 Repair costs experienced by the 6-storey archetype building at (a) IM1, (b) IM7 and (c) IM8

V. RESULTS

For each Intensity Measure (IM), building losses obtained from the 500 realizations have been sorted in ascending order to enable the calculation of the probability that total loss is less

(or greater) than a specific value l_t. At this stage of the analysis, the total loss threshold has been set equal to 0.4 RepC. Just to give an idea, Figs. 3, 4 show the repair costs recorded for the 8R building (Fig. 3) and 6A building (Fig. 4) at (a) IM1 (T_R=30 years), (b) IM7 (T_R=475 years), (b) IM8 (T_R=975 years), disaggregated in contributions from six component categories. Realizations in which either collapse occurs or residual drifts exceed the limit of reparability are summarized in Table VII (data relevant to the 6A building are in parenthesis).

As expected, the component categories that contribute most to the building losses are masonry infills, partitions and partition-like, on average by 50% and 25%, respectively, at IM7 for both buildings. At this seismic intensity, the contribution of structural components does not exceed 15%. Generally speaking, the same trend is observed also at the other seismic intensities, with economic losses related to structural repair that became negligible for seismic intensities lower than IM5.

TABLE VII
NUMBER OF REALIZATIONS ASSOCIATED WITH BUILDING REPLACEMENT

IM	MAFE	Sa(T*) (g)	Collapse	Repairability 1 (exceeding residual drift limit)	Repairability 2 (exceeding loss threshold)
1	3.28%	0.046 (0.049)	0 (1)	0 (0)	0
2	1.98%	0.061 (0.064)	1 (4)	0 (0)	0 (2)
3	1.38%	0.073 (0.077)	1 (10)	0 (0)	0 (1)
4	0.99%	0.088 (0.092)	3 (6)	0 (0)	42 (31)
5	0.71%	0.105 (0.110)	4 (28)	0 (0)	84 (60)
6	0.50%	0.126 (0.132)	17 (38)	0 (0)	94 (103)
7	0.21%	0.192 (0.201)	56 (131)	10 (11)	216 (216)
8	0.10%	0.263 (0.275)	126 (231)	22 (1)	333 (213)
9	0.04%	0.385 (0.403)	254 (-)	82 (-)	163 (-)

Fig. 5 shows the cumulative probability distributions of exceedance a given economic loss, for each IM for the (a) 8R and (b) 6A building. The broken vertical line identifies the total loss threshold (assumed equal to the 40% of the replacement cost of the building, i.e. 952.000 and € 557.000 € for 8R and 6A building, respectively), beyond which the replacement of the building is deemed more convenient than repairing and the total loss is assumed equal to the replacement cost of the building and, as consequence, the probability of exceedance becomes constant. Considering the seismic intensities between IM1 and IM3 for the 8R building (see Fig. 5 (a)), the probability of exceedance becomes constant and equal to zero before the attainment of the building loss threshold, meaning that the building is always repairable. The probability of exceedance associated with the attainment of the building loss threshold increases from 9% to 96%, passing from IM4 to IM8. For IM9, the probability of exceedance is always 100%, meaning that the building is never conveniently repairable from an economic point of view. On the other hand, for the 6A building, the building is always repairable only for IM1 seismic intensity (see Fig. 5 (b)) while the probability of exceedance associated with the attainment of the building loss threshold increases from 2% to 90% passing from IM2 to IM8.

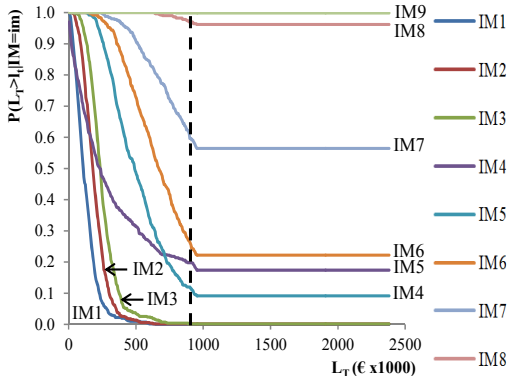

(a)

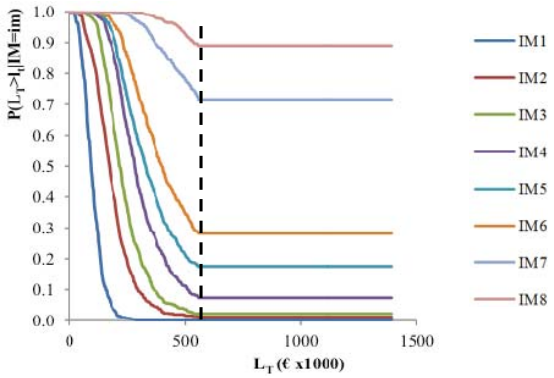

(b)

Fig. 5 Cumulative probability distributions of exceedance a given economic loss for each IM relevant to (a) 8R and (b) 6A building

Time-based performance assessment is accomplished with the evaluation of the building loss curve, (see Fig. 6), which plots the total expected losses (in this study related to building repair only), as a function of the annual probability of exceedance of repair cost of different amounts. The building loss curve is derived assembling the results of the intensity-based performance assessment for each IM (see Fig. 5) with the hazard curve of the building site (see Fig. 2). Fig. 6 shows the buildings loss curve of the 8R and 6A building models, respectively, disaggregated into contributions from each IM.

By combining the building losses expected in a sequence of possible earthquake scenarios with the mean annual frequency of exceedance of each scenario, the so-called building Expected Annual Loss (EAL) is obtained, which represents an estimate of the average economic loss, due to earthquake damage, that accrues every year in the building [9]. From a graphical point of view, EAL is given by the area underneath the loss curves of Fig. 6. Table VIII shows the expected

annual loss (EAL) of the four building models examined in this study. In the last column Table VIII, the values of EAL are normalized by the Replacement Cost (RepC) of the building.

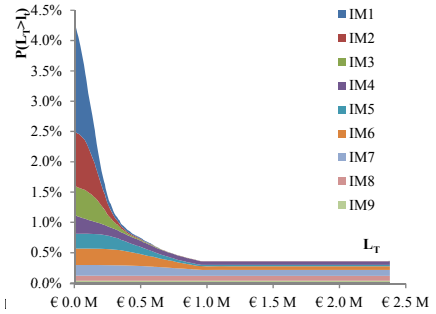

(a)

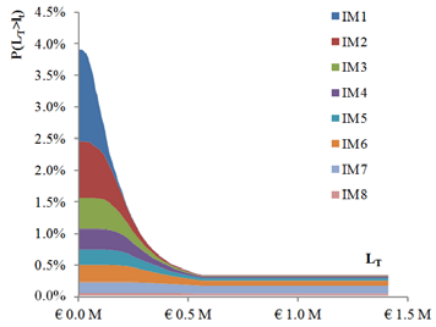

(b)

Fig. 6 Building loss curve of (a) 8R and (b) 6A building model

TABLE VIII
EXPECTED ANNUAL LOSS OF THE SELECTED BUILDINGS

Case study	RepC	EAL	EAL_{RepC}
8R	2.380.000 €	17.878 €	0.75 %
	1.520.000 €	16.190 €	1.07 %
4A	927.655 €	8.534 €	0.92%
6A	1.390.000 €	12.316 €	0.89 %
8A	1.855.311 €	15.213 €	0.82%

To determine the influence of the main analysis parameters involved in the evaluation of EAL, a sensitivity analysis has been carried out. In particular, the influence of the following parameters has been investigated: (i) total loss threshold, (ii) damage correlation, (iii) modeling dispersion and (iv) collapse spectral acceleration.

As far as the total loss threshold is concerned, four different percentages of RepC have been considered, namely: 40% (initial choice), 50%, 70% and 100% (i.e. no threshold). Increasing the total loss threshold from 40% to 100%, EAL decreases (on average) less than 15% (see Table IX).

Performance groups can be designated as having either correlated or uncorrelated damage. Correlated damage means that all components within a performance group will always have the same damage state. If a performance group is designated as uncorrelated, then each component of the performance group can experience a different damage state. In this study the default choice was uncorrelated damage. Assuming correlated damage within each storey, EAL slightly increases, e.g. from 0.75 to 0.8% of RepC for the 8R building.

As far as the modeling dispersion is concerned, assuming the maximum and minimum values of β_m recommended in PACT (equal to 0.57 and 0.14, respectively), EAL changes a little, e.g. from 0.7% to 0.78% of RepC for the 8R building.

Changing the median value of the spectral acceleration at collapse does not affect significantly EAL, due to choice of imposing a cap on the level of repair effort at which a building is likely to be replaced rather than repaired.

TABLE IX
VARIABILITY OF EAL WITH TOTAL LOSS THRESHOLD (TH)

Case study	TH = 40%	TH = 50%	TH = 70%	TH = 100%
8R	0.75%	0.67%	0.62%	0.61%
4A	0.92%	0.84%	0.80%	0.79%
6A	0.89%	0.83%	0.78%	0.78%
8A	0.82%	0.77%	0.72%	0.71%

VI. COMPARISON WITH PAST APPLICATIONS

The normalized values of EAL obtained with PACT for the buildings under scrutiny have been compared with those derived from past PEER-PBEE applications to old RC frame buildings representative of the US building stock (see Table X). They include the Van Nuys Hotel, a 7-storey RC perimeter moment-resisting frame building, characterized by deformed bars as steel reinforcement; exterior glazing and interior drywall as main non-structural components, built in 1966 in Van Nuys (California), and a set of 26 archetype "non–ductile" office building structures, with number of storeys ranging from 2 to 12, featuring either perimeter or space RC frames characterized by deformed bars as steel reinforcement; exterior glazing and interior drywall as main non-structural components, designed by [11] using the 1967 Uniform Building Code.The main features of the Van Nuys Hotel and non-ductile archetype buildings are summarized Table X and compared with those of the residential buildings examined in this study. Although all these buildings may be simply labeled as pre-70 RC frame buildings, significant differences, in terms of structural characteristics, non-structural components and soil type, exist, which must be taken into account in the comparison of results.

Results are compared in Table XI. For consistency, the attention is focused on the 8-storey buildings only. The differences in the results relevant to the Van Nuys Hotel are mainly due to differences in the number of damageable components considered in the seismic assessment and the manner in which repair costs were computed. For that reason, the results of the study by [9] have been neglected.

As can be seen, despite inevitable differences in the assumptions regarding damage states, fragility groups and repair costs, the final results of past PBEE applications to old RC frame buildings are quite consistent, pointing out values of EAL ranging from 1.36% to 2.2% of the replacement cost of

the building. At a glance, the values of EAL obtained in this study seem to be a little lower.

TABLE X
PAST APPLICATIONS TO OLD RC FRAME BUILDINGS

Building ID	Description	Structural type	Non-structural elements	Bay width (m)	Soil Type (*)
Van Nuys Hotel (California)	19 x 46 m 3 x 8 bays 7 storeys Built in 1965	Perimeter RC frame with 2-way RC flat slabs. Use of deformed bars. Non ductile details.	Exterior glazing; Interior drywall; Suspended ceilings;	5.75 6.10	C
Archetype Non-Ductile Office Buildings (California)	38 x 53(38) m 4 x 4 bays 2-4-8-12 storeys Built in 1967.	(i) Perimeter RC frame with 2-way RC flat slabs; (ii) RC space-frame with RC joist slabs. (iii) Use of deformed bars. (iv) Non ductile details.	Exterior glazing; Interior drywall; Acoustic ceilings.	7.25	C
Residential Buildings (Italy)	12(15) x 27 m 3 x 7 bays 8 storeys Built in 1965.	RC frame with RC joist slabs. Use of plain bars. Non ductile details.	Exterior masonry infills; Interior masonry partitions.	2.75 4.30	A

(*) According to the European Seismic code [10]

TABLE XI
COMPARISON WITH RESULTS OF PAST APPLICATIONS ON OLD RC BUILDINGS

Reference	Building Description	Soil Type	Numerical Model	EAL_{RepC}
[8]	Van Nuys Hotel (7 storeys)	C	2D bare frame	0.77 %
[12]	Van Nuys Hotel (7 storeys)	C	2D bare frame	2.2 %
[13]	Van Nuys Hotel (7 storeys)	C	2D bare frame	1.6%
[14]	Van Nuys Hotel (7 storeys)	C	2D bare frame	1.36%-1.63%
[11]	Non-ductile Office buildings (8 storeys)	C	2D bare frame	1.8%-2.1%
[15]	Non-ductile Office buildings (8 storeys)	C	2D bare frame	1.8 % - 2.2%
[7]	Non-ductile Residential buildings (8 storeys)	A	3D infilled frame	0.75%-1.07%

The aforesaid discrepancies can be ascribed to the following issues:

- Use and occupancy classification of the building (i.e. residential vs. hotel or office), which implies substantial differences in terms of fragility groups, especially for what concerns non-structural components. The selection of damageable assemblies and the definition of the associated fragility parameters, indeed, drastically affect the results.
- Structural characteristics, see third column of Table X.
- Numerical model (2D bare frame models vs. 3D infilled frame models), see fourth column of Table X.
- Collapse Mechanism. Indeed, the behavior of the buildings examined in this study cannot be defined as "non-ductile", in the sense that collapse mechanism is not governed by column sway mechanisms or premature brittle shear failure. Indeed, a fairly good ductility capacity is found, due to the formation of plastic hinges in beams before joint failure.
- Seismic hazard (Los Angeles area, California, vs. L'Aquila, Italy).
- Use of Conditional Mean Spectra (CMS) instead of Uniform Hazard Spectra (UHS). Indeed, previous research has shown that scaling up arbitrarily selected ground motions to a specified target spectral acceleration (like in the UHS) can produce overly conservative structural responses, because a single extreme level of Sa(T) does not imply occurrence of equally extreme Sa(T) levels at all periods [8].
- Soil type (C vs. A). In this regard, preliminary analyses assuming soil type C (instead of soil type A) have been carried out on the selected case study buildings, leading to an increase of EAL of the order of 35%.
- Rugged components. A number of structural and non-structural components, including staircase and elevator, have been assumed as rugged, thus neglecting the associated loss contributions.
- Unit repair costs. The repair costs considered in this study for the development of loss functions are different from those assumed in past studies, being derived from different sources, relevant to different building construction industries (Italy vs. US).
- Replacement Cost. The manner in which the replacement cost of the building is calculated (e.g. as construction cost of a new building with similar characteristics using current costing manuals, or as present value of the original construction cost) affects the estimation of EAL.

VII. CONCLUSIONS

In this paper, the performance seismic assessment methodology proposed in FEMA P-58 has been applied to a number of case studies represented by typical RC frame buildings realized in Italy (and other European countries) before 70s (i.e. before the introduction of seismically oriented codes). The selected building was designed for gravity loads only, using low-strength concrete and plain steel reinforcing bars. It features non-structural masonry walls as exterior infills and internal partitions.

Specific tools for the performance seismic assessment of these buildings have been first developed. They include a number of fragility curves for different damage states of the main structural and non-structural components (i.e. exterior and interior beam-column joints, ductile weak columns and masonry infills with and w/o openings) and the associated loss functions, accounting for repair costs that would be required to

restore each component to its pre-earthquake (essentially undamaged) condition. The proposed fragility curves and loss functions have been implemented in the Performance Assessment Calculation Tool (PACT) of FEMA P-58. Time-based performance assessment has been performed with PACT, to estimate seismic losses for the selected building.

First, pushover analysis has been performed to evaluate collapse fragility curves. Next, comprehensive nonlinear response-time history analyses have been carried out, to evaluate seismic response at different earthquake hazard level. PACT has been then used to estimate the Expected Annual Loss (EAL) of the building, which represents the amount one could expect to pay, on average, every year to repair earthquake damage, considering different sources of uncertainties.

Values of EAL of the order of 0.75-1% (considering stiff soil) and 1-1.4% (considering soft soil) of the Replacement Cost of the selected buildings have been found, which turns out to be consistent with results of past PBEE applications on old RC frame buildings representative of the US building stock, considering the differences in structural characteristics, seismic hazard, numerical modeling, damage states, fragility groups and repair costs.

Another interesting result of this study comes from the disaggregation of EAL into different loss contributions. As expected, large part (approximately 80%) of the building loss is due earthquake damage to non-structural components (masonry infills, partitions and partition-like components). As a consequence, future studies on this class of buildings shall focus on improving the accuracy and reliability of fragility curves and loss functions for masonry infills, partitions and partition-like components.

Performance seismic assessment with FEMA P-58 is very demanding from a computational point of view, as it requires extensive nonlinear response history analyses to predict the seismic response of the structure. From this point of view, the development of simplified procedures, for a reliable estimate of the seismic response of the building, within the FEMA P-58 framework, would be very useful.

REFERENCES

[1] ATC - Applied Technology Council, *FEMA P-58: Next-generation Seismic Performance Assessment for Buildings, Volume 1 – Methodology*, Federal Emergency Management Agency, Washington, D.C., 2012.

[2] D. Cardone, and G. Perrone, ''Developing fragility curves and loss functions for masonry infill walls'', *Earthquakes and Structures*, Vol. 9(1), pp. 257-279, 2015.

[3] D. Cardone, "Fragility curves and loss functions for RC structural components with smooth rebars," *Earthquakes and Structures*, Vol. 10(5), 2016. DOI: http://dx.doi.org/10.12989/eas.2016.10.5.000.

[4] CIAMI - Collegio degli ingegneri e degli architetti di Milano, Prezzi tipologie edilizie, Edited by DEI, Roma, Italy, pp. 500 (in Italian), 2014.

[5] S. Pampanin, M. Moratti, G.M. Calvi, "Seismic Behaviour of R.C. Beam-Column Joints Designed for Gravity Loads," *12th European Conference on Earthquake Engineering, London*, 2002.

[6] L. Decanini, F. Mollaioli, A. Mura, and R. Saragoni, "Seismic performance of masonry infilled R/C frames", *13WCEE,* Vancouver, Canada, 2004.

[7] D. Cardone, and G. Perrone, "Performance-based earthquake engineering of pre-70 RC buildings," in "Displacement-based Loss Assessment of existing structures pre- and post-seismic rehabilitation," *First year Report of Reluis/DPC 2014/2017 research project*, IUSS Press, Pavia, Italy, 2015.

[8] J.W. Baker, "Conditional Mean Spectrum: Tool for ground motion selection." *Journal of Structural Engineering*, vol. 137(3), pp. 322–331, 2011.

[9] K.A. Porter, J.L. Beck, R.V. Shaikhutdinov, "Simplified performance-based earthquake engineering estimation of economic risk for buildings", *Earthquake Spectra*, vol. 20(4), pp. 1239-1263, 2004.

[10] CEN - Comité Europeen de Normalization, *Eurocode 8: Design of Structures for Earthquake Resistance - Part 1: General rules, seismic actions and rules for buildings*, CEN, Brussels, Belgium, PrEN 1998-1: 2005.

[11] A.B. Liel, and G.G. Deierlein, "Assessing the collapse risk of California's existing reinforced concrete frame structures: metrics for seismic safety decisions," *Technical Report No. 166*, John A. Blume Earthquake Engineering Center, Stanford University, 2008.

[12] H. Krawinkler, "Van Nuys Hotel Building Testbed Report: Exercising Seismic Performance Assessment", *PEER Report 2005/11*. Pacific Earthquake Engineering Research Center, Berkeley, CA., 2005.

[13] H. Aslani, and E. Miranda, "Probabilistic Earthquake Loss Estimation and Loss Disaggregation in Buildings", *Report No. 157*, John A. Blume Earthquake Engineering Center, Stanford University, 2005.

[14] M. Baradaran Shoraka, T.Y. Yang, and K.J. Elwood, "Seismic Loss estimation of non-ductile reinforced concrete buildings", Earthquake Eng. Struct. Dyn, Vol. 42, 297-310, 2013.

[15] C.M. Ramirez, and E. Miranda, "Building specific loss estimation methods & tools for simplified performance-based earthquake engineering," *Technical Report No. 171*, John A. Blume Earthquake Engineering Center, http://blume.stanford.edu, Stanford University, 2009.